



## Structural and thermal investigations of a Tunisian natural phosphate rock

Hassen Bachouâ<sup>1</sup>, Masseoud Othmani<sup>1</sup>, Yannick Coppel<sup>2</sup>, Nabil Fatteh<sup>3</sup>,  
Mongi Debbabi<sup>1</sup>, Béchir Badraoui<sup>1,4</sup>

<sup>1</sup> *Laboratoire de Physico-chimie des Matériaux, Faculté des Sciences de Monastir, 5019 Monastir, Tunisie*

<sup>2</sup> *CNRS, LCC (Laboratoire de Chimie de Coordination), 205 route de Narbonne, BP 44099, F-31077 Toulouse Cedex 4, France*

<sup>3</sup> *Centre de recherches CPG Mélaoui 2134 Gafsa, Tunisie*

<sup>4</sup> *Institut Préparatoire aux Etudes d'Ingénieur de Monastir, 5019 Monastir, Tunisie*

Received 2 Jan 2014, Revised 8 May 2014, Accepted 8 May 2014

\* Corresponding author. E mail: [badraoui\\_b@yahoo.fr](mailto:badraoui_b@yahoo.fr); Tel +(216)73500273

### Abstract

Tunisian natural phosphate rock from M'dhilla deposits are characterized by different methods. The principal constituent of the phosphate rock sample is the carbonate fluoroapatite phase to which other clay and siliceous mineral; sulfates, carbonates and organic matter are associated. The crystallographic structure of natural phosphate was examined by powder X-Ray diffraction (XRD) at different temperatures of calcinations. The XRD diagrams show a significant structure change with increasing of the temperature to 1100 °C. The MAS-NMR technique was used to study the carbon, phosphorus, silicon and fluoride environment. The result confirms the single phosphate apatitic phase; the NMR study also indicates the presence of a small amount of organic compounds which was detected by chemical analysis (only 0.6%), IR spectroscopy and thermogravimetric analysis.

*Keywords:* Phosphate rock; Francolite; X-Ray diffraction; MAS-NMR

### Introduction

Phosphates are of great importance in Tunisia for agriculture, industry and exports. Production is about 6 to 7 MT annually and exports about 2 MT. About 20% of foreign currency comes from this sector. Tunisia occupies the fifth rank among producing countries. Sedimentary phosphate minerals are generally crystalline [1]. The structure and the chemical composition of phosphate are vary widely with the origin of deposits and are mainly composed of apatite in association with a wide assortment of accessory minerals, mainly fluorides, carbonates, quartz, silicates, sulfates and organic material [2].

In this paper, a characterization of a sample from M'dhilla deposit has been made to determine his morphological, chemical and structure characteristics and thermal stability. The characterization techniques used are chemical analysis, X-ray diffraction (XRD), infrared spectroscopy Fourier transform (FT-IR), Scanning Electron Microscopy (SEM) coupled with the Dispersive analysis I energy of X-ray (EDX), specific surface area measurement (SSA), high-resolution MAS-NMR, thermogravimetric analysis (TGA) and differential thermal analysis (DTA).

## 2. Experimental procedure

### 2.1 Experimental

The phosphate rock sample chosen in this study originated from M'dhilla region (Tunisia). Samples were provided by the services of Gafsa Phosphates Company (CPG). The starting materials were washed with water, dried at 110°C overnight and sieved to give a size fraction between 100 and 400 µm using ASTM sieves, according to the protocol used in the research centre of CPG. The sample was crushed for homogenization.

### 2.1. Materials and Methods

The characterization of materials was performed by many physical-chemical analyses. Elemental analyses were performed at Gafsa Phosphates Company (CPG-Tunisia), the lead and cadmium concentrations were determined

with a Perkin Elmer 3110 atomic absorption spectrophotometer and the phosphate ions were quantified by visible absorption spectrophotometry of the phosphovanadomolybdic complex using Varian Cary50Bio spectrophotometer [3]. The chemical analysis of the carbon has been determined according to the Anne method [4]. X-Ray powder diffractograms were obtained at room temperature on a Panalytical X'Pert PRO MPD equipped with copper anticathode tube. The identification of the phases was carried out using the standard data base ICDD-PDF2004. Infrared spectra were recorded at resolution from 400 to 4000  $\text{cm}^{-1}$  on a BRUKER EQUINOX 55 Fourier transform spectrometer using KBr pellets. SEM/EDX was used to investigate the morphology of the prepared samples. Measurements were taken on a Philips FEI Quanta 200 scanning electron microscope in the conventional high-vacuum mode. The specific surface areas (SSA) measurements were carried out by BET-method (adsorptive gas  $\text{N}_2$ , carrier gas He, heating temperature 150 °C using sorptometer EMS-53 and KELVIN 1040/1042 (Costech International). Thermogravimetric analysis (TGA) and differential thermal analysis (DTA) of the sample were performed in the air flow at a heating rate of 10°C/min in a Pt crucible with SETARAM SETSYS 1750 equipment. Solid-state NMR experiments were recorded on a Bruker Advanced 400 spectrometer equipped with a 4 mm probe. Samples were spun at 8 kHz or 12 kHz (for  $^{19}\text{F}$ ) at the magic angle using  $\text{ZrO}_2$  rotors. For  $^1\text{H}$  MAS,  $^{13}\text{C}$  MAS,  $^{19}\text{F}$  MAS,  $^{29}\text{Si}$  MAS and  $^{31}\text{P}$  MAS single pulse experiments, small flip angle ( $\sim 30^\circ$ ) were used with recycle delays of 5s, 5s, 10s, 60s and 20s, respectively.  $^{13}\text{C}$ ,  $^{29}\text{Si}$  and  $^{31}\text{P}$ -NMR spectra were recorded under high-power proton decoupling conditions. All chemical shifts for  $^1\text{H}$ ,  $^{13}\text{C}$  and  $^{29}\text{Si}$  are relative to TMS.  $^{19}\text{F}$  and  $^{31}\text{P}$  were referenced to  $\text{CFCl}_3$  and 85%  $\text{H}_3\text{PO}_4$ , respectively.

### 3. Results and Discussion

#### 3.1 Chemical analysis

The chemical composition of the natural phosphate rock is presented in *Table 1*. The principal constituents of the phosphate rock sample are the fluoroapatitic phase to which other clay and siliceous mineral, sulphates, carbonates and organic matter are associated. Other elements with negligible amounts were detected. It is important to note that the atomic ratio  $\text{Ca/P} = 2.17$  is close to stoichiometric value for francolite [2].

**Table 1:** Chemical composition of Tunisian natural phosphate

Element	Ca	P	F	C <sub>org</sub>	Si	S	Mg	Al	Ca/P
Composition	34.86%	12.83%	2.92%	0.60%	1.45%	1.26%	0.51%	0.27%	2.17

#### 3.2 X-ray diffraction

A powder X-ray diffraction (XRD) analysis was used to determine the crystalline phases of the Tunisian natural phosphates rocks. In order to obtain further information on the modification of the phosphate rock structure induced by thermal treatment, the samples were treated at different temperatures in the range 100 - 1100°C. All the DRX diagrams show a good resolution of the peaks of XRD, which proves a good crystallinity of the sample (Figure 1). Therefore, the diffractograms show that the majority of the lines are attributable to the apatitic phase.

The unit cell parameters and crystallite size calculated for powders natural phosphates rock are reported in *Table 2*.

**Table 2:** The unit cell parameters (Å) and crystallite size calculated for powders Tunisian natural phosphate

a(Å)	c(Å)	$\beta_{1/2}$ (002)	$D_{002}$ (Å)	$\beta_{1/2}$ (310)	$D_{310}$ (Å)
9.337	6.887	0.194	420	0.268	309

Unit cell parameters are calculated from XRD lines, using Celref program [5]. The values of the crystallite size were calculated using Debye–Scherrer equation with X'Pert High Score Pus program [6]:

$$D = \frac{K\lambda}{\beta_{1/2} \cos \theta}$$

Where D is the value of crystallite size (nm),  $\lambda$  is the wavelength of monochromatic X-ray beam ( $\lambda = 1.5418 \text{ \AA}$  for  $\text{CuK}\alpha$  radiation),  $\theta$  is the diffraction angle ( $^\circ$ ), K is a fixed constant equal to 0.9 for apatite crystallites and  $\beta_{1/2}$  is line width at half maximum of a given reflection (rad) calculated with WinPLOTR program.

The significant increase of the parameter  $a = 9.337 \text{ \AA}$  compared to francolite ( $a = 9.34 \text{ \AA}$ ,  $c = 6.88 \text{ \AA}$ ) (00-002-0833, ICDD-PDF) is probably due to substitutions, explaining the high reactivity of the Tunisian natural phosphate rock, which justify the industrial interest, despite the low relative  $\text{P}_2\text{O}_5$  amount.

It can be seen clearly from the figure that the phosphate rock sample is carbonated apatite. This result is confirmed by the value of  $2\theta$  at 23.3 and 28.34° ( $2\theta$ ) [7]. It should also be noted in the spectra of the sample treated at 100°C that there is no trace of the broad signals at 15-25° ( $2\theta$ ) of organic material [8]. The organic material is present in quantities too small to be detected by X-rays. This is confirmed by chemical analysis. The crystalline phases obtained after the treatment of the sample up 600°C are reported in Table 3.

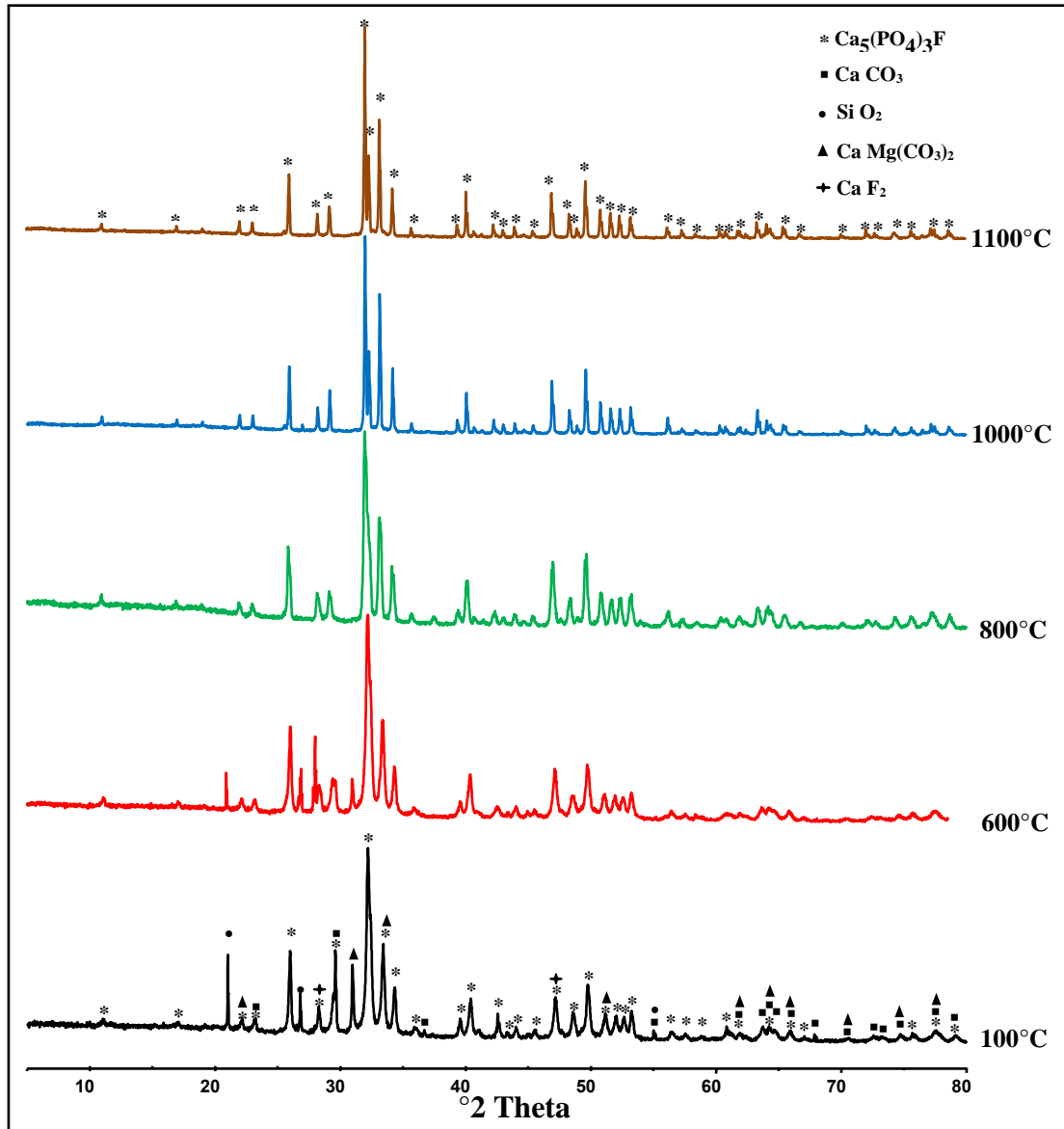


**Figure 1:** Diagrams of diffraction X-rays of phosphate rock at various calcinations temperatures

**Table 3:** Compounds of phosphate rock

Compounds	2 Theta (°2θ)
<b>Francolite</b>	25.864 - 31.937 - 32.268 - 33.128 - 34.142 - 46.866 - 49.584
<b>Fluorite</b>	28.340 - 47.125
<b>Calcium carbonate</b>	29.624 - 36.297 - 39.759 - 43.541 - 47.833 - 48.887
<b>Dolomite</b>	30.953 - 41.145 - 50.529
<b>Quartz</b>	21.042 - 26.809 - 55.019

At 800°C, and above all signals are attributable to the apatitic phases. The values of unit cell in different temperature are presented in table 4. These results confirmed that, on strong heating, francolite changes to fluorapatite with loss of CO<sub>2</sub>.

**Table 4:** The unit cell parameters (Å) and crystallite size calculated for powders Tunisian natural phosphate heated for 4h at different temperatures

Temperatures (°C)	100	600	800	1100	FAp*
<i>a</i> -axis (Å)	9.337	9.339	9.368	9.372	9.367
<i>c</i> -axis (Å)	6.887	6.871	6.884	6.880	6.884

\* File 00-015-0876, ICDD-PDF

### 3.2 IR spectroscopy

The infrared spectrum of the sample is (Figure 2). The spectrum is characterized by a number of typical absorption bands found in other natural or synthetic apatitic phosphates [9-13].

The groups of bands at 966, 1045 and 1097  $\text{cm}^{-1}$  are ascribable to symmetrical and anti-symmetric elongations of  $(\text{PO}_4)^{3-}$  groups. Other bands are ascribable to the symmetrical and anti symmetric deformations of  $(\text{PO}_4)^{3-}$  groups (474, 578 and 605  $\text{cm}^{-1}$ ) [14]. The bands appearing at 867, 1430 and 1457  $\text{cm}^{-1}$  characterizes carbonate ions  $(\text{CO}_3)^{2-}$ , agreeing with the values usually reported in literature of the B-type carbonate [15] and in accordance with unit cell parameters are calculated from XRD lines.

The present of B-type carbonate bands and the absence of characteristic bands of hydroxyl ions  $\text{OH}^-$  (630 and 3560  $\text{cm}^{-1}$ ) confirm that this phosphate is francolite B-type [15] in which  $\text{CO}_3$  groups substituted  $\text{PO}_4$ . Water absorption bands can be observed at 1646 and 3427  $\text{cm}^{-1}$ . The bands appearing in the domain 750 and 815  $\text{cm}^{-1}$  can be due to the vibration of silicates groups [16].

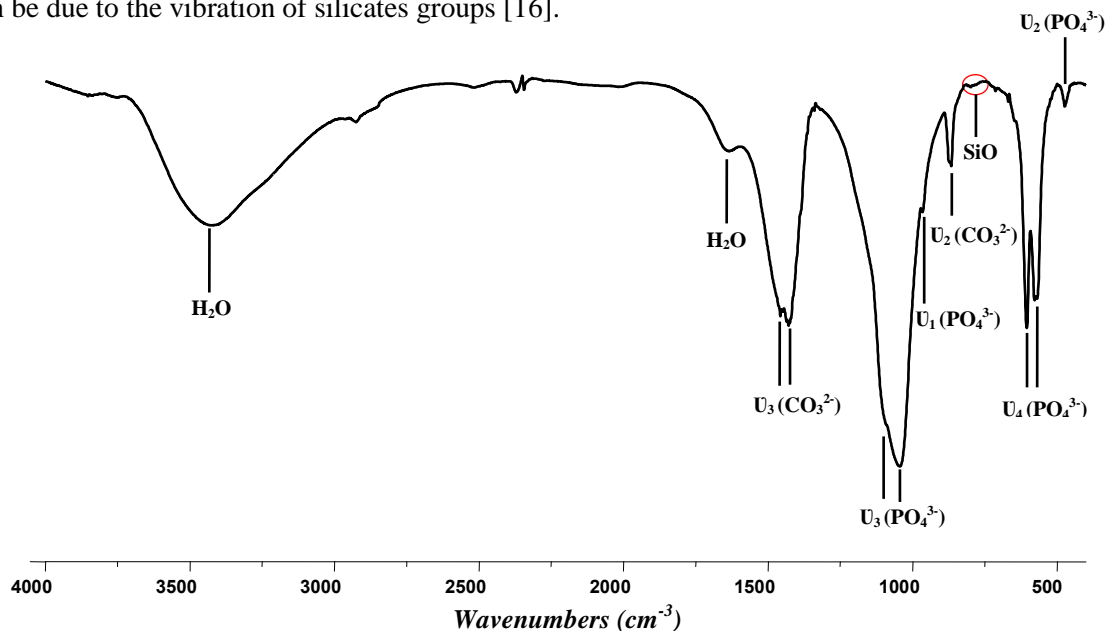


**Figure 2:** Infra-red spectrum of rock phosphate dried at 100°C

### 3.4. SEM and EDX of rock phosphate

The observation under the scanning electron microscopy (SEM) (Figure 3) shows that the morphology of phosphate rock is made mainly by particles of irregular forms. Other particles are related to the presence of the organic remainders and quartz grains. Coupled with the dispersive analysis in energy of X-rays (EDX) (Figure 4) is chow the presence of Ca, P, O, Si, C, F and traces of other elements. This observation confirmed the results found by XRD, IR and chemical analysis.

### 3.5. Specific surface area measurement

A specific surface area measurement of the phosphate rock, by the Brunauer-Emmett-Teller (B.E.T.) method, give a value of 20.70  $\text{m}^2/\text{g}$ , indicating, that natural phosphate has a low porosity compared with synthetic apatitic with values superiors of 120  $\text{m}^2/\text{gr}$  [17,18].

The isotherm of adsorption-desorption of nitrogen with the phosphate rock is illustrated in Figure 5, which is of type IV according to Brunauer classification [19].

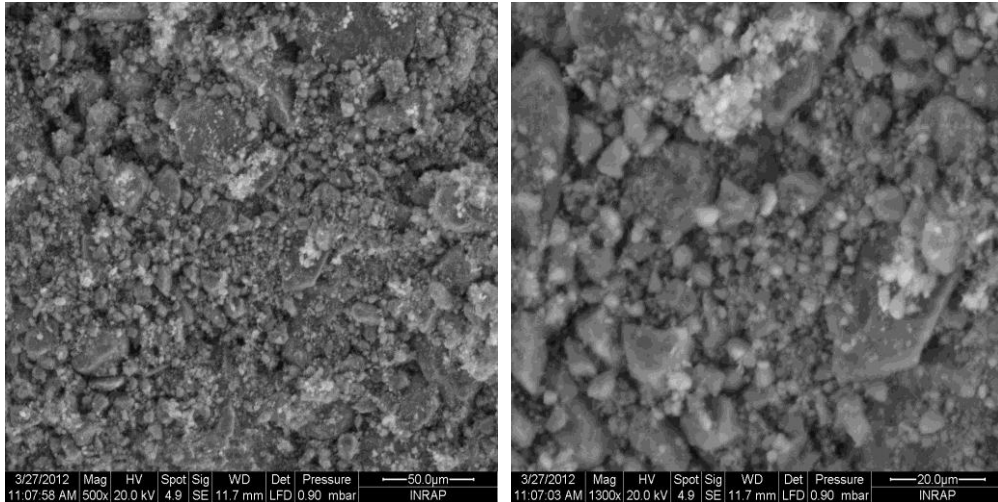


Figure 3: Images of SEM of the Rock Phosphate particles with two different resolutions

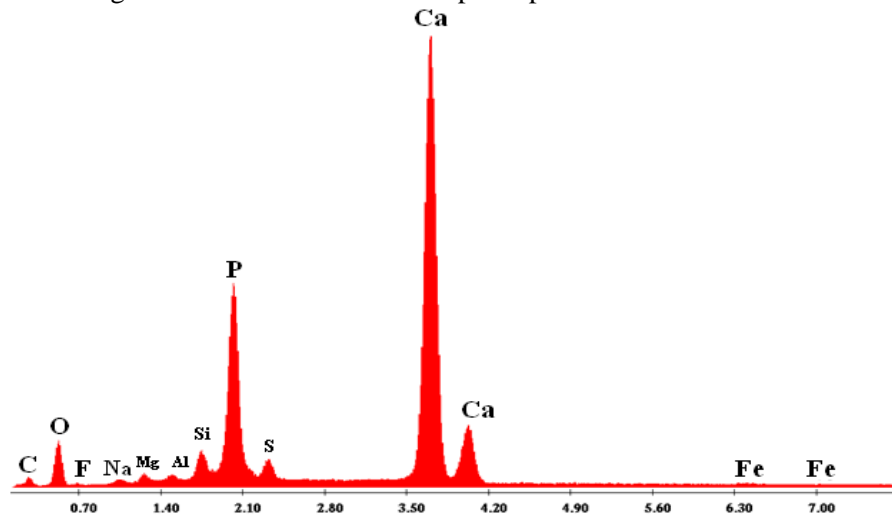


Figure 4: EDX analysis of phosphate rock

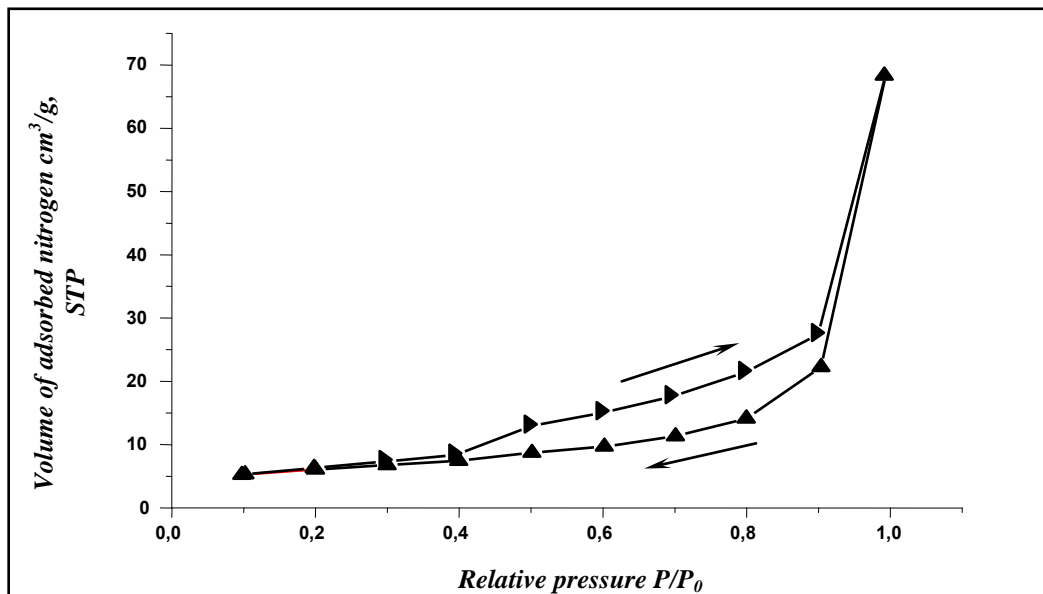
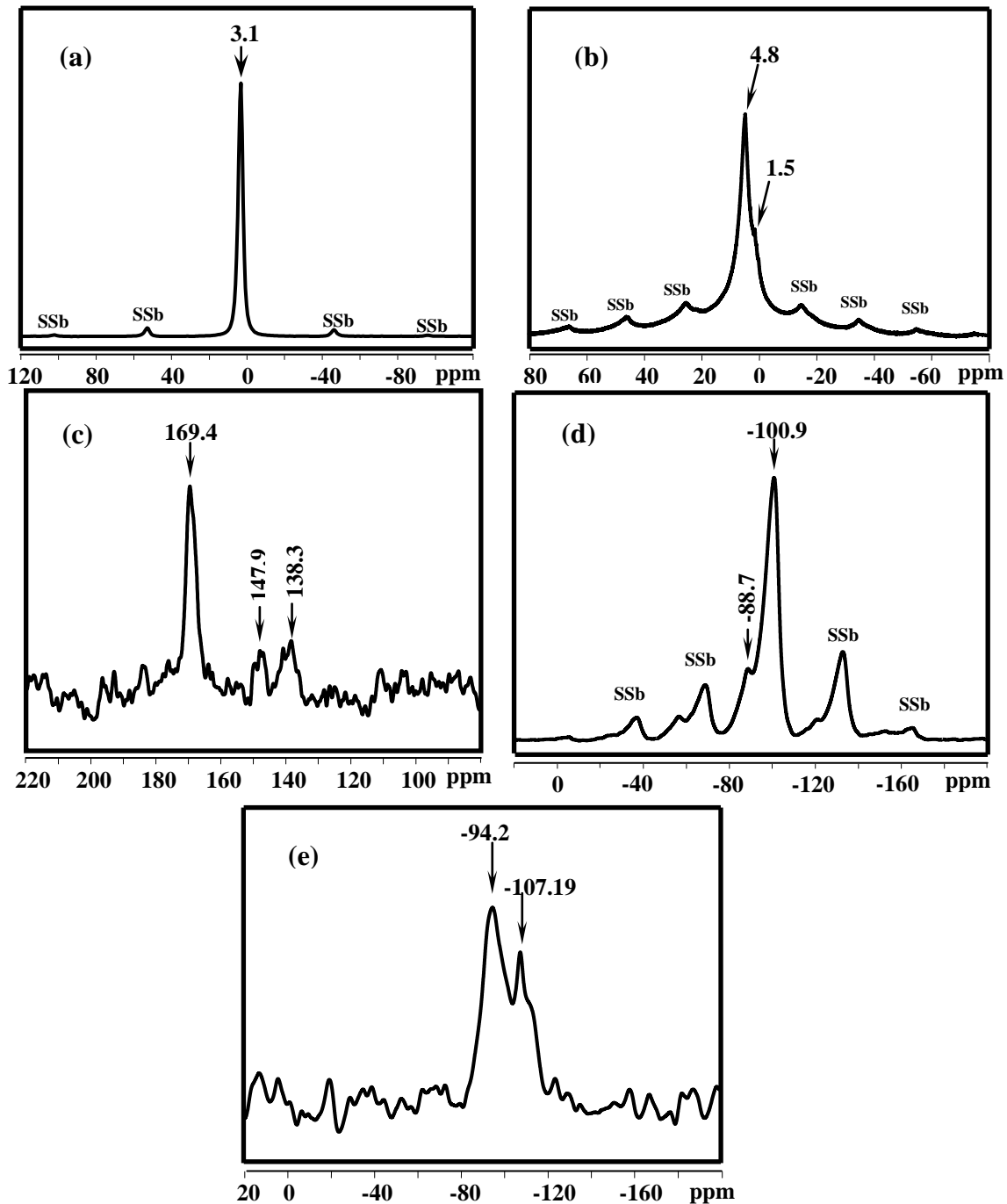


Figure 5: Isotherms of adsorption and desorption of nitrogen by of phosphate

### 3.6. MAS-NMR spectra

Nuclear magnetic resonance spectroscopy is a technique for studying the immediate chemical environment around certain atoms. One of the most important advantages of solid-state NMR is the ability to observe directly some elements in their chemical environment in the sample under study, irrespective of whether the sample is crystalline or not.

The solid state  $^{31}\text{P}$  MAS-NMR spectra of the Tunisian natural phosphate rock are depicted in Figure 6 (a) and present a central resonance at  $\delta_{\text{iso}} = 3.1$  ppm associated with spinning side bands pattern, characteristic of the chemical-shift anisotropy (CSA) of the phosphorus nucleus. The single peak observed for phosphorus, confirms the presence of a single phosphate apatitic crystalline [20, 21].



**Figure 6:**  $^{31}\text{P}$  MAS-NMR (a),  $^1\text{H}$  MAS-NMR (b),  $^{13}\text{C}$  MAS-NMR (c),  $^{19}\text{F}$  MAS-NMR (d),  $^{29}\text{Si}$  MAS-NMR (e) spectra of phosphate rock.

Two signals are observed in the  $^1\text{H}$  MAS-NMR spectra (Figure 6 (b)), at 1.47 ppm and at 4.69 ppm, respectively characteristics of OH groups and  $\text{H}_2\text{O}$  molecules adsorbed on the surface [22]. The  $^{13}\text{C}$  MAS-NMR spectrum of the phosphate rock is shown in Figure 6 (c). The resonance with high intensity at 169.4 ppm indicates the presence of carbonate ( $\text{CO}_3$ )<sub>2</sub> species. The two small broad peaks at 147.9 and 138.3 ppm confirm the presence of small amount of organic compounds. The  $^{19}\text{F}$  MAS-NMR spectrum of Tunisian natural phosphate (Figure 6 (d)), shows two broad peaks at -100.9 and -88.7 ppm, ascribable respectively to fluoroapatite [23] and fluorite  $\text{CaF}_2$  [24]. The examination of spectra  $^{29}\text{Si}$  MAS-NMR in Figure 6 (e) shows two peaks, at -107.1 ppm characteristic of the presence of quartz  $\text{SiO}_2$  [25] and at -94.2 ppm characteristic of the presence of phosphosilicate apatite [26]. NMR is thus useful in giving structural information which may not be obtained from XRD, either because the material does not give sharply resolved diffraction peaks or because phases are present in quantities too small to be detected by XRD.

### 3.7. Thermal analysis

Thermal stability study of phosphates rock were carried out using thermo gravimetric analysis (TGA) and differential analysis (DTA) from room temperature to 1100°C (Figure 7).

The TGA curve of the phosphate studied indicates a first weight loss of 0.52% between 25°C and 250°C corresponding to the desorption of water. A second mass loss of 1.65% between 250°C and 450°C corresponds to the elimination of organic matter [27]. The last weight loss of 5.38% between 450°C and 1100°C is attributed to the decomposition of mineral carbonates present in the phosphate as indicated by IR., XRD and  $^{13}\text{C}$  MAS-NMR.

The DTA curve showed the presence of an endothermic effect at 147°C attributed to the evaporation of adsorbed water onto phosphate surface and two exothermic peaks at 360°C and 697°C respectively attributed to combustion of organic matter and decomposition of carbonates.

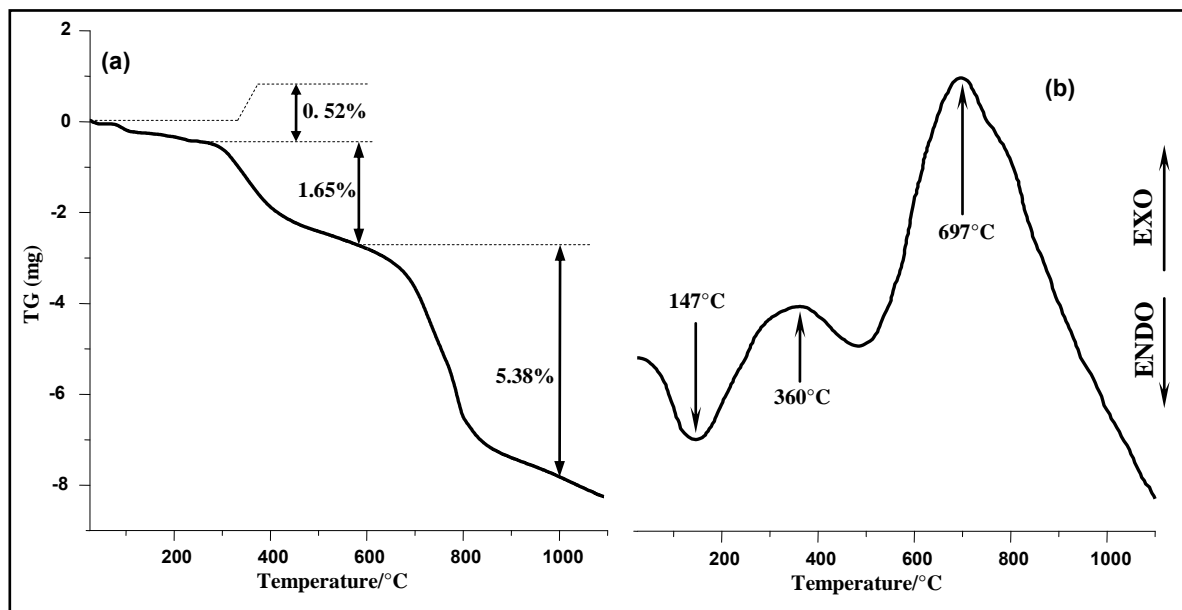


Figure 7: TGA (a) and DTA (b) curves of phosphate rock

### Conclusion

The aim of this work was to conduct a detailed structural and physical-chemical study characterizing the Tunisian phosphate rock from M'dhilla deposits. The XRD and IR results indicate that the major constituent of the sample is B-type carbonate-fluoroapatite (Francolite).  $^{31}\text{P}$ ,  $^{13}\text{C}$  and  $^{19}\text{F}$  MAS-NMR spectroscopy identified the carbonate environments associated with three mineral components of the sample (calcite, fluorite and a carbonate-fluoroapatite).

The  $^{29}\text{Si}$  MAS-NMR indicates the presence of  $\text{SiO}_2$  quartz and silicates in the sample, confirming the results of chemical analysis. Thermal analysis indicates the decomposition of carbonate-fluoroapatite, from 800°C, giving fluoroapatite.

**Acknowledgments** - We are thankful the Company of Phosphate Gafsa (CPG) for providing the investigated phosphate sample, the INRAP (Institut Nationale de Recherche et d'Analyses Physico-chimiques), the RTCEn (Research and Technology Centre of Energy) and the University of Monastir (Tunisia). We are very grateful to Mr HADROUG Ali for the linguistic help.

## References

1. Ben Hassen A., Trichet J., Disnar J. R., Belayouni H., *Swiss Journal Geoscience* 3 (2010) 457.
2. M. Feki, *Contribution à la purification de l'acide phosphorique de voie humide par extraction à la méthylisobutylcétone*, Thesis, University of Tunis (2001).
3. Quinlan K.P., De Sesa M.A., *Analytical Chemistry* 27 (1955) 1626.
4. Hénin S., Dupuis M., *Ann. Agron.*, 1 (1945) 17.
5. Altermatt U. D., Brown I. D. A., *Acta Cryst A.* 43 (1987) 125.
6. Bigi A., Boanini E., Capuccini C., Gazzano M., *Inorganica Chimica Acta.* 360 (2007) 1009.
7. Nadiri A., Dhibi D., Bentayeb A., Bih L., Maghnoij J., *Phosphorus Research Bulletin* 15 (2004) 35.
8. El ouardi M. *Étude de la calcination du phosphate clair de youssoufia (Maroc)*, *Afrique science* 04 (2008) 199.
9. El Asri S., Laghzizil A., Alaoui A., Saoiabi A., M'Hamdi R., El Abbassi K., Hakam A., *Journal of Thermal Analysis and Calorimetry* 95 (2009)15.
10. Elliott J.C., *Structure and Chemistry of the Apatites and Other Calcium Orthophosphates*, Elsevier: Amsterdam (1994).
11. Othmani M., Aissa A., Goze Bac C., Rachdi F., Debbabi M., *Applied Surface Science* 274 (2013) 151.
12. Othmani M., Aissa A., Bachoua H., Debbabi M., *Applied Surface Science* 264 (2013) 886.
13. Turki T., Othmani M., Bantignies J. L., Bouzouita K., *Applied Surface Science* 290 (2014) 327.
14. El Hammari L., Synthèse et études physico-chimiques des phosphates de calcium poreux greffés par des molécules organiques : *Structure et processus d'adsorption*, Mohamed V- Agdal University, (2007).
15. Perrone J., Fourest B., Giffaut E., *Journal of Colloid and Interface Science*, 249 (2002) 441.
16. Aguiar H., Serra J., González P., León B., *Journal of Non-Crystalline Solids* 355 (2009) 475.
17. Errassifi F., *Mécanisme d'adsorption du risedronate par des phosphates de calcium biologiques : Application aux biomatériaux*, Cadi Ayyad University, (2011).
18. Verwilghen C., Rio S., Nzihou A., Gauthier D., Flamant G., Sharrock P. J., *J. Mater. Sci.* 42 (2007) 6062.
19. Lowell S., Shields S. J., Thomas M.A., Thommes M., *Characterization of Porous Solids and Powders: Surface Area, Pore Size and Density*, Elsevier, 2006, pp. 13.
20. Jäger C., Walzel T., Zaika W. M., Epple M., *Magn. Reson. Chem.* 44 (2006) 573.
21. Rothwell W.P., Waugh J.S Yesinowski., J.P., *J. Am. Chem. Soc.* 102 (1980) 2637.
22. Yesinowski J. P., Hellmut E., *J. Am. Chem. Soc.* 109 (1987) 6274.
23. Zainuddin N., Karpukhina N., Law R. V., Hill R. G., *Dental Materials* 28 (2012) 1051.
24. Chen H., Sun K., Tang Z., Law R. V., Mansfield J. F., Clarkson B. H., *American Chemical Society* 6 (2006) 1504.
25. Fiske P. S., William J. N., Xu Z., Stebbins J. F., *American Mineralogist* 83 (1998) 1285.
26. Sakamoto M., Yanaba Y., Morita K., *Journal of Non-Crystalline Solids*, 358 (2012) 615.
27. Groune K., Halim M., Benmakhlof M., Arsalane S., Lemee L., Ambles A., *J. Mater. Environ. Sci.* 4 (4) (2013) 472.

(2015) ; <http://www.jmaterenvirosci.com/>